Available online at www.eccomasproceedia.org
Eccomas Proceedia COMPDYN (2023) 2261-2270

ECCOMAS
Proceedia

COMPDYN 2023
9th ECCOMAS Thematic Conference on
Computational Methods in Structural Dynamics and Earthquake Engineering
M. Papadrakakis, M. Fragiadakis (eds.)
Athens, Greece, 12-14 June 2023

SEISMIC RETROFITTING OF FRAMED STRUCTURES BY DAMPED BRACES CONSIDERING THE OUT-OF-PLANE RESPONSE OF MASONRY INFILLS

Fabio Mazza[1] **and Rodolfo Labernarda**[2]

[1] Dipartimento di Ingegneria Civile, Università della Calabria
Ponte P. Bucci, 87036, Rende (Cosenza), Italy
e-mail: fabio.mazza@unical.it

[2] Dipartimento di Ingegneria Civile, Università della Calabria
Ponte P. Bucci, 87036, Rende (Cosenza), Italy
rodolfo.labernarda@unical.it

Abstract

Design procedures of hysteretic damped braces (HYDBs) for the seismic retrofitting of buildings are generally focused on the in-plane (IP) behaviour of masonry infills (MIs) while neglecting their out-of-plane (OOP) response. Ex-post checking on effectiveness of the HYDBs against the OOP seismic collapse of MIs is generally made. To overcome this limitation, a displacement-based design procedure of HYDBs is updated by including the effects of the OOP nonlinear seismic response of MIs. Specifically, the retrofit design target displacement is derived from the capacity curve of the original infilled structure, in which IP and OOP contributions of MIs parallel and perpendicular to the direction of seismic loads are considered, respectively. To this end, a computer code for the nonlinear static analysis of spatial framed structures is enhanced introducing a five-element macro-model of a MI, composed of a central IP truss element and four diagonal OOP beams that govern its inelastic response. Modal and uniform load distributions are considered, proportional to the floor masses and the concentrated OOP mass of MIs. A five-storey reinforced concrete hospital building with regular plan and elevation is preliminarily designed in a medium-risk seismic zone. Bare and infilled structural models are examined, the latter including MIs in the interior bays of the perimeter frames. Then, retrofitting of the test structures in a high-risk seismic zone is carried out, incorporating diagonal steel braces with HYDs in the perimeter frames of the building plan. Finally, nonlinear dynamic analyses are performed before and after retrofit to delve further into the reliability of the HYDBs, also including nonlinear IP and OOP response of MIs.

Keywords: Reinforced Concrete Buildings, Hysteretic Damped Braces, In-Plane Response of Masonry Infills, Out-of-Plane Response of Masonry Infills, Nonlinear Static Analysis.

ISSN:2623-3347
Peer-review under responsibility of the organizing committee of COMPDYN 2023.
doi: 10.7712/120123.10558.20679

1 INTRODUCTION

Unreinforced masonry infills (MIs) are widely used as exterior enclosure of existing reinforced concrete (RC) framed buildings, although they highlighted during past earthquakes an extensive in-plane (IP) and out-of-plane (OOP) damage with economic losses that far exceeded the structural damage [1]. Moreover, these nonstructural elements may induce closure of public buildings such as hospitals in the aftermath of an earthquake, forcing evacuation of patients, and lowering of their performance levels. The IP and OOP nonlinear seismic response of MIs has been recently studied, combining single or multiple IP struts with fibre-section and beam/truss OOP models [2]. In the present work, a simplified five-element macro-model of MIs [2], taking into account the IP (i.e. compression at the centre, compression at the corners, shear sliding and diagonal tension) and OOP (i.e. falling debris) failure modes that can occur in the infill panels during an earthquake, is implemented in a C++ computer code for the nonlinear static analysis of infilled framed structures [3]. A trilinear IP backbone curve of a MI is calculated and kept constant during seismic analysis [4], while a bilinear OOP backbone curve is assigned adopting lower (FEMA 356, [5]) and upper (Dawe & Seah, [6]) bound formulations for the OOP maximum strength.

The aim of the present work is to explore the effectiveness of an upgraded version of a displacement-based design procedure of hysteretic damped braces [7,8], considering not only the structural safety of the framed structure, but also the seismic protection of IP drift-sensitive and OOP acceleration-sensitive MIs. The test structure is represented by a five-storey RC pavilion of the hospital campus in Avellino (Italy), characterized by a symmetrical plan with MIs placed in the two internal bays along the X direction and the central bay along the Y one of the perimeter frames. A simulated design of the test structure is preliminarily carried out in line with provisions of a former Italian seismic code (DM96, [9]), assuming a strategic function after an earthquake. Nonlinear static analyses of bare (BS) and infilled (IS) framed structures are carried out along the principal axes of the building plan, considering the IP and OOP nonlinear force-displacement law of MIs parallel and perpendicular to the direction of seismic loads. Structural and nonstructural performance points are identified referring to four structural damage targets and IP and OOP collapse of MIs. Bare (RBS) and infilled (RIS) retrofitted structures are designed for a high-risk seismic zone by hysteretic damped braces (HYDBs) placed in such way to avoid bays with MIs. Nonlinear dynamic analyses of the original (BS and IS) and retrofitted (RBS and RIS) hospitals are carried out, with reference to serviceability (SDE) and Basic (BDE) artificial accelerograms [10], corresponding to operational and life-safety seismic intensity levels provided by the current Italian code (NTC18, [11]).

2 ORIGINAL TEST STRUCTURES

A five-storey RC pavilion of the hospital campus in Avellino, Campania (Italy), is selected as test structure [7], characterized by four frames along the X direction and five along the Y one, and 4.0 m storey height (Figure 1). The structure is partially infilled with MIs placed in the interior bays of the perimeter frames, characterized by the lowest (i.e. $L_X/h=1$) and highest (i.e. $L_Y/h=1.75$) values of the aspect ratio (i.e. width-to-height ratio). The vertical loads are represented by 7.93 kN/m^2 on the top floor and 10.23 kN/m^2 on the other floors, while an additional load of 5.5 kN/m is considered on the perimeter beams corresponding to the infilled bays. A cylindrical compressive strength of 25 N/mm^2 and a yield strength of 450 N/mm^2 are considered for concrete and steel reinforcement, respectively. A simulated design of the bare framed building is carried out in compliance with DM96 [9], assuming medium-risk seismic zone and typical subsoil class. Specifically, structural design is carried out at the ultimate limit state considering MIs as nonstructural elements, while the IP drift ratio threshold imposed

by DM96 (i.e. Δ/h, with Δ interstorey drift and h storey height) is assumed equal to 0.4% for limiting nonstructural damage at the serviceability limit state. Interior flat beams are oriented parallel to the floor slab direction, while all the others are deep beams; square and rectangular cross-sections are considered for the interior and exterior columns, respectively. Further details can be found in a previous paper by Mazza [7].

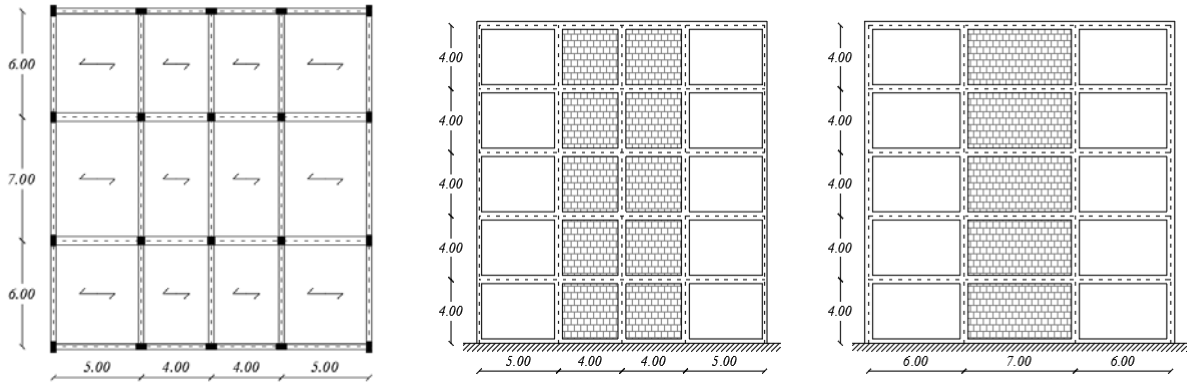

(a) Plan (X-Y). (b) Elevation (X-Z). (c) Elevation (Y-Z).

Figure 1: Layout of the Avellino (Italy) hospital (unit in metres) and arrangement of MIs.

A five-element model describes the IP-OOP nonlinear interaction of a MI [2,4], comprising four diagonal OOP beam elements connected to a horizontal central IP truss element by means of two nodes where the OOP mass corresponding to the first mode of vibration is lumped (i.e. $m^{(OOP)}=0.81m_{MI,tot}$, $m_{MI,tot}$ being the total mass of the panel). Specifically, four spherical hinges are considered to the connection joints of the OOP beam elements with the frame, while two cylindrical hinges at the end sections of the IP truss element. The initial stiffness and maximum lateral strength ($F_{max}^{(IP)}$) of the horizontal strut are calculated on the basis of the Mainstone [12] and Bertoldi et al. [13] formulations, respectively, assuming a mean height of the infill panels h_w=3.2 m. Trilinear IP backbone curves for MIs of the infilled structure are reported in Figure 2a, assuming different levels of lateral force: i.e. initial cracking, $0.4F_{max}^{(IP)}$; full cracking, $F_{max}^{(IP)}$; residual strength, $0.7F_{max}^{(IP)}$. Note that IP backbone curves refer to the total thickness (i.e. t_w=24 cm) of the infill panel constituted of two identical layers made with hollow bricks. Further details can be found in a previous paper [4].

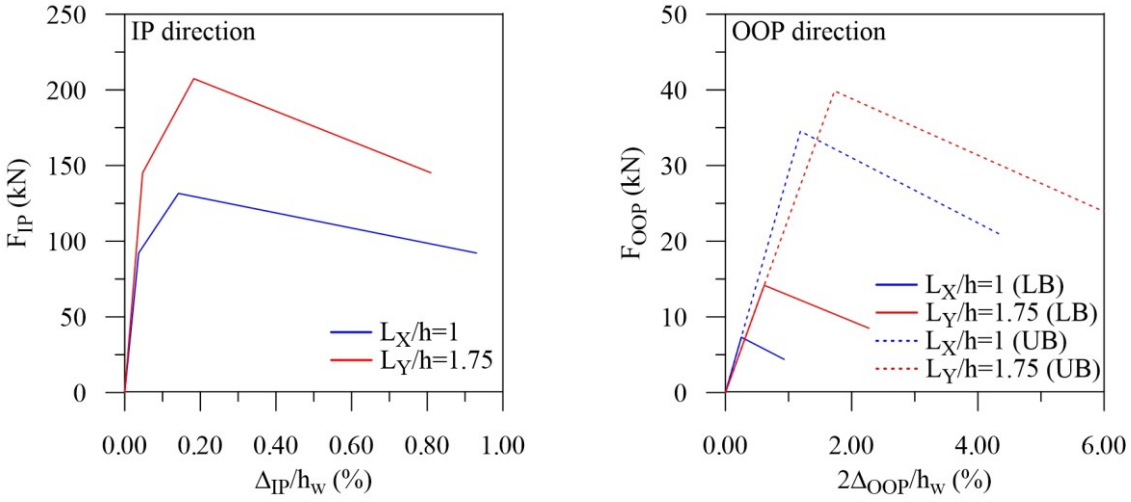

(a) In-plane (IP) response. (b) Out-of-plane (OOP) response.

Figure 2: Force-displacement laws for MIs of the Avellino (Italy) hospital.

Bilinear OOP backbone curves are also plotted in Figure 2b, considering two characteristic points: i.e. full arching action, $F_{max}^{(OOP)}$; residual strength, $0.6F_{max}^{(OOP)}$. The maximum OOP strength is evaluated according to lower-bound (LB) one-way [5] and upper-bound (UB) two-way [6] arching formulations available in the literature, similarly to the IP variability of materials and geometrical infill properties [14], while the initial and post-cracking stiffnesses are kept constant. Main dynamic properties of bare (BS) and infilled (IS) structures are reported in Table 1: i.e. two main vibration periods and corresponding effective masses, along the in-plan principal directions, expressed as a percentage of the corresponding total mass.

Structure	$T_{1,X}$	$T_{1,Y}$	$m_{1,X}$ (% m_{tot})	$m_{1,X}$ (% m_{tot})
BS	0.677 s	0.574 s	75.25	74.56
IS	0.597 s	0.532 s	76.74	75.87

Table 1: Dynamic properties of the hospital structures: m_{tot}=2369 t.

Pushover curves of the BS along the X and Y principal directions are plotted in Figure 3, representing the roof drift ratio (i.e. d_{top}/H_{tot}, d_{top} and H_{tot} being the horizontal top displacement and total height) versus normalised base shear (i.e. V_{base}/W_{tot},W_{tot} being the total seismic weight). Constant gravity loads are applied together with invariant distributions of lateral loads monotonically increasing and proportional to the floor masses, with (i.e. "modal") and without (i.e. "uniform") considering the contribution of the first (elastic) vibration mode.

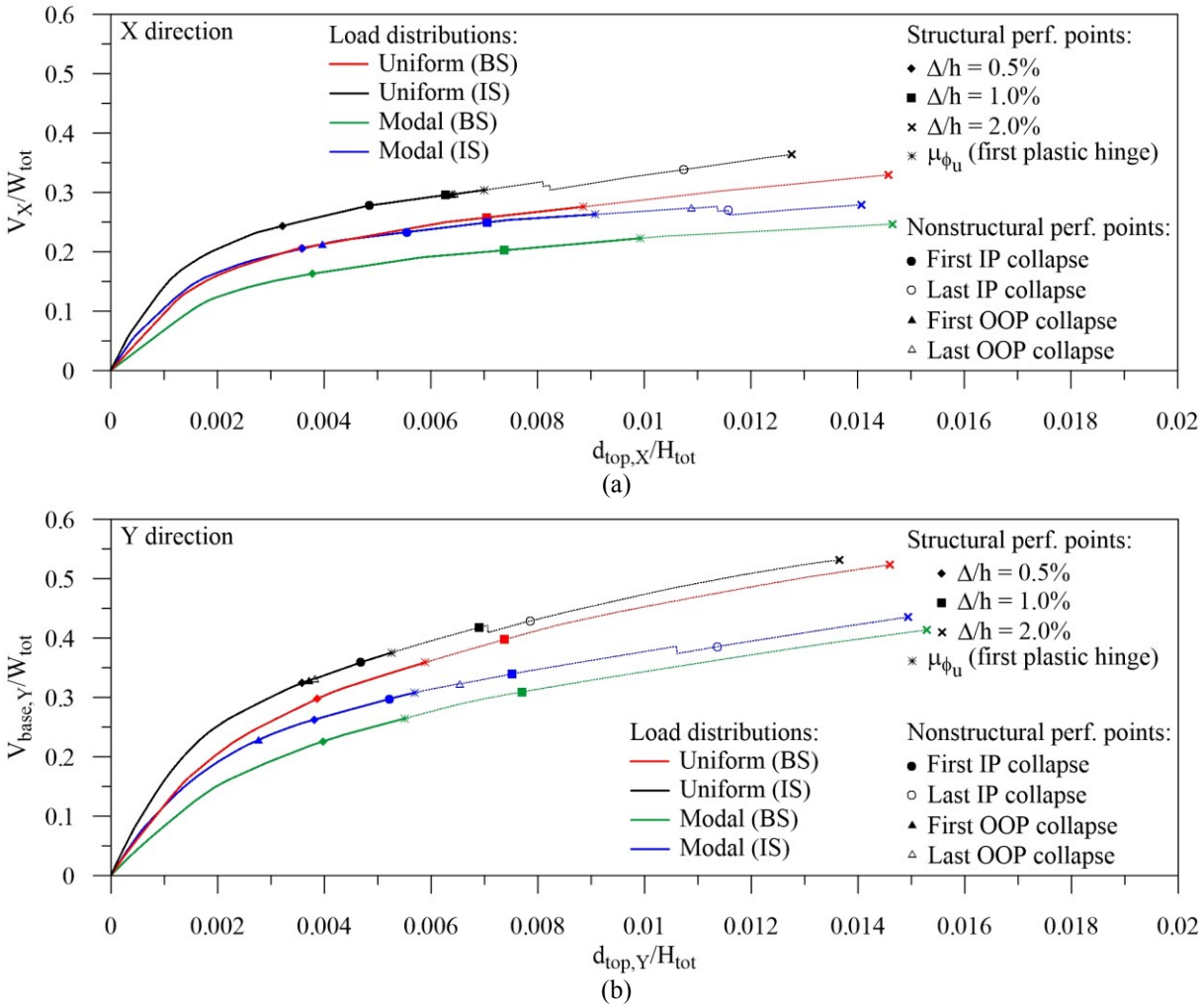

Figure 3: Pushover curves of the bare (BS) and infilled (IS) original hospital structures.

A lumped plasticity model with piecewise linearization of the axial load-biaxial bending moment elastic domain is used in order to describe the inelastic behaviour of the RC frame members [3], while the IP and OOP contribution of MIs parallel and perpendicular to the direction of the seismic loads, respectively, is also considered for the IS [2,4]. Specifically, the modal distribution of the IS structure includes the OOP mass of the infill panels multiplied by a coefficient increasing along the building height with the same law of the acceleration provided by the European seismic code for the OOP verification of MIs [15]. It should be noted that the IP↔OOP nonlinear mutual interaction of MIs is not triggered because of the symmetrical building plan. Four structural damage thresholds are considered, three in terms of interstorey drift ratio (i.e. Δ/h=0.5%, 1% and 2%) and the last corresponding to the attainment of the ultimate value of curvature ductility demand at critical end sections of the frame members, evaluated in accordance with the provisions of the NTC18 for existing buildings [11]. Moreover, performance points corresponding to the first and last IP and OOP collapse of MIs for the lower bound formulation shown in Figure 2b are also highlighted for the IS structure. In the seismic retrofitting with HYDBs, attention will be focused on the modal capacity curves exhibiting minimum value of the V_{base}/W_{tot} ratio.

3 RETROFITTED TEST STRUCTURES

The seismic retrofitting of the original test structure is carried out by the insertion of diagonal hysteretic damped braces (HYDBs), with in-plan arrangement and vertical distribution shown in Figures 4a and 4b,c, respectively. A high-risk seismic zone (i.e. peak ground acceleration on rock, a_g=0.5 g) and moderately-soft subsoil (i.e. class C, site amplification factor S=1.0) are assumed at the collapse prevention limit state. A reference time period V_R=200 years (obtained by multiplying the nominal structural life V_N=100 years by a coefficient of use c_U=2) is imposed considering NTC18 provisions for hospitals.

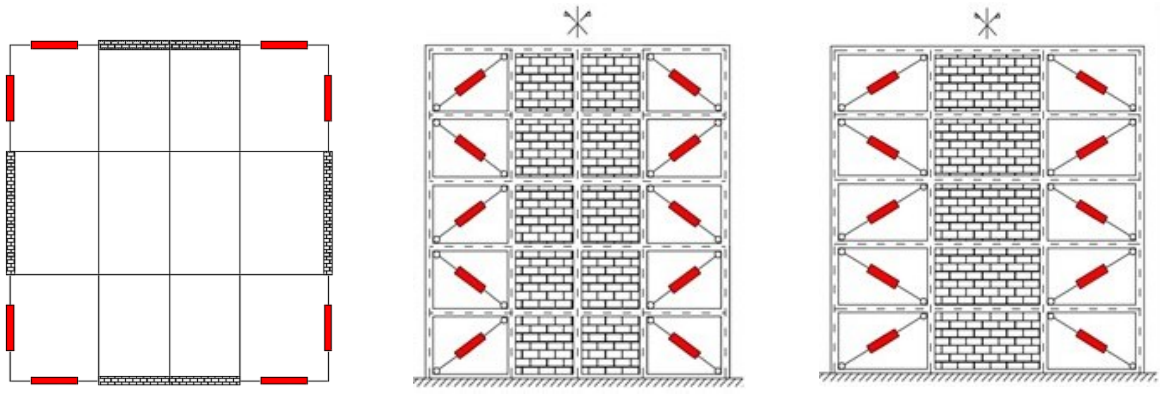

(a) Plan (X-Y). (b) Elevation (X-Z). (c) Elevation (Y-Z).

Figure 4: Layout of the HYDBs for the Avellino (Italy) hospital (unit in metres).

A four-step displacement-based design (DBD) procedure of HYDBs proposed in previous works [7,8] is improved considering the influence of the IP and OOP nonlinear modelling of MIs on the selection of optimal properties of the HYDBs. First, nonlinear static analysis of the original bare and infilled framed structures is carried out assuming two in-elevation configurations of MIs with lower bound formulation of their IP (Figure 2a) and OOP (Figure 2b) force displacement laws when HYDBs are designed: i.e. retrofitted bare structure (RBS), with nonstructural MIs; retrofitted infilled structure (RIS) with a uniform in-elevation distribution of MIs. Then, the DBD procedure of the HYDBs is applied for attaining a designated perfor-

mance level in terms of a target displacement: i.e. top displacement corresponding to an interstorey drift ratio equal to Δ/h=0.5%, for the RBS; the minimum value between top displacement corresponding to Δ/h=0.5% and first OOP collapse of a MI, for the RIS. In-elevation distribution laws of total lateral stiffness (K_{DB}) and yield shear (V_{yDB}) for HYDBs of the RBS and RIS retrofitted structures are reported in Table 2, assuming the following design parameters: i.e. ductility demand of the HYDBs, μ_{DB}=20; stiffness hardening ratio of the HYDBs, r_{DB}=3%; hardening ratio of the frame, r_F=5%.

	RBS				RIS			
Floor	$K_{DB,X}$	$V_{yDB,X}$	$K_{DB,Y}$	$V_{yDB,Y}$	$K_{DB,X}$	$V_{yDB,X}$	$K_{DB,Y}$	$V_{yDB,Y}$
5	1963971	874	1544214	782	1542625	789	2386261	764
4	2915557	1888	2427368	1671	3827521	1664	3506755	1652
3	3888777	2640	3345497	2317	3675625	2378	4720289	2313
2	5255810	3092	4891025	2698	4758169	2818	6427647	2714
1	9205384	3279	7820543	2865	8243544	3002	10398086	2890

Table 2: Stiffness and strength properties of the HYDBs for the retrofitted structures (units in kN and m).

4 NUMERICAL RESULTS

Four structural configurations are examined with reference to the interior layout of MIs in the perimeter frames (Figure 1), with and without exterior arrangements of HYDBs in the building plan (Figure 4): i.e. bare (BS) and infilled (IS) original (before retrofitting) hospitals; bare (RBS) and infilled (RIS) retrofitted hospitals. Dynamic analysis of the test structures is carried out by means of nonlinear modelling of all nonstructural and structural parts: i.e. MIs with the five-element macromodel described in previous works [2,4]; RC frame members with a lumped plasticity beam element, considering piecewise linearization of the axial load-biaxial bending moment elastic domain at the end sections where inelastic deformations are expected [3]; HYDBs, with truss elements characterized by a bilinear force-displacement law with ultimate value of ductility equal to 25, without considering the flexibility of the supports. A 5% and 2% of elastic viscous damping ratio is also assumed for the BS and IS, respectively, in line with the Rayleigh approach. As prescribed by EC8 [15], the first damping coefficient corresponds to the fundamental vibration period, while the second one refers to the vibration period corresponding to a sum of the effective modal masses exceeding 95% of the total mass. Two sets of biaxial artificial accelerograms are generated by using the computer code SeismoArtif [10], with reference to serviceability (SDE) and basic (BDE) earthquakes corresponding to the seismic intensity levels provided by NTC18 [11]. Each set consists of three couples of accelerograms whose acceleration (elastic) response spectra match on average the design spectrum at 5% of linear viscous damping ratio.

First, maximum values of the IP drift ratio of MIs, defined as the IP interstorey displacement ($\Delta_{max,IP}$) normalized by storey height of the infill panels (h_w), are shown in Figures 5a and 5b for operational and life-safety limit states, respectively. Attention is focused on the lower bound formulation of the force-displacement law of MIs reported in Figure 2a. At each storey, $\Delta_{max,IP}$ is evaluated at the minimum instant of time between that corresponding to the IP and OOP collapses of MIs and the final instant of simulation in the case of no collapse. Curves refer to the original (IS, red line) and retrofitted (RIS, blue line) infilled structures. As can be observed, the RIS satisfies DM96 threshold (i.e. $\Delta_{max,IP}/h_w$=0.4%) at SDE (Figure 5a) and collapse threshold (i.e. $\Delta_{u,IP}/h_w$=0.75%) at BDE (Figure 5b), while they are exceeded at the intermediate floor levels of the IS. Graphs similar to the previous ones are reported in Figure 6 with reference to maximum values of the OOP drift ratio, evaluated as the mean displacement of both nodes where the OOP mass of an infill panel is lumped ($\Delta_{max,OOP}$)

normalized by half of the infill height ($h_w/2$). The original structure does not exceed the FEMA 356 threshold with respect to seismic loads at both SDE (Figure 6a) and BDE (Figure 6b). On the other hand, the insertion of the HYDBs has not always beneficial on the OOP response of MIs for the retrofitted structures, with high OOP demand mainly localised at the top level where the FEMA 356 threshold is exceeded for both intensity levels. This threshold is never exceeded when an alternative retrofitted structure is considered (i.e. RIS*, green line), assuming that upper bound OOP values of the maximum strength and ultimate displacement of MIs are adopted while HYDBs designed for lower bound values are kept constant.

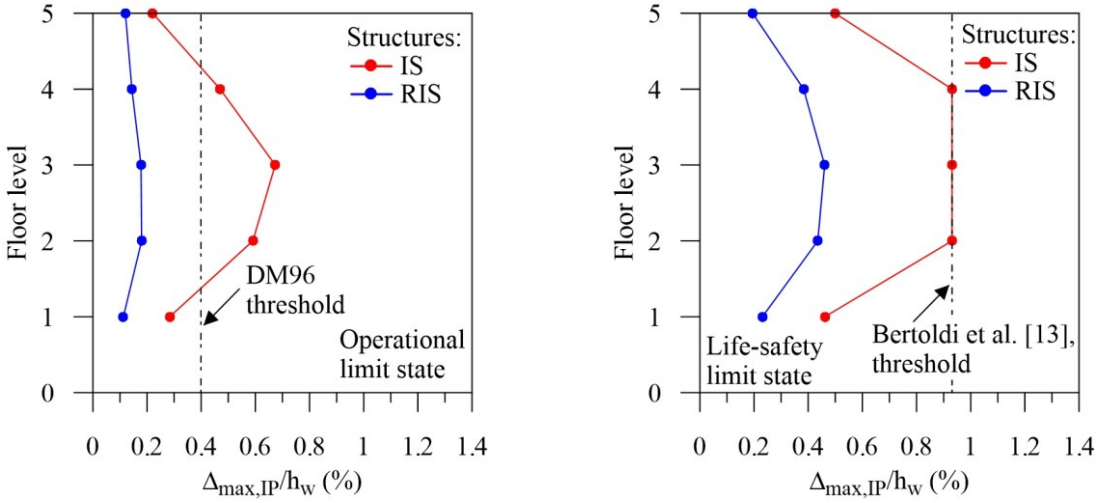

(a) SDE. (b) BDE.

Figure 5: Maximum IP drift ratio of MIs for the original (IS) and retrofitted (RIS) hospitals at serviceability and ultimate limit states.

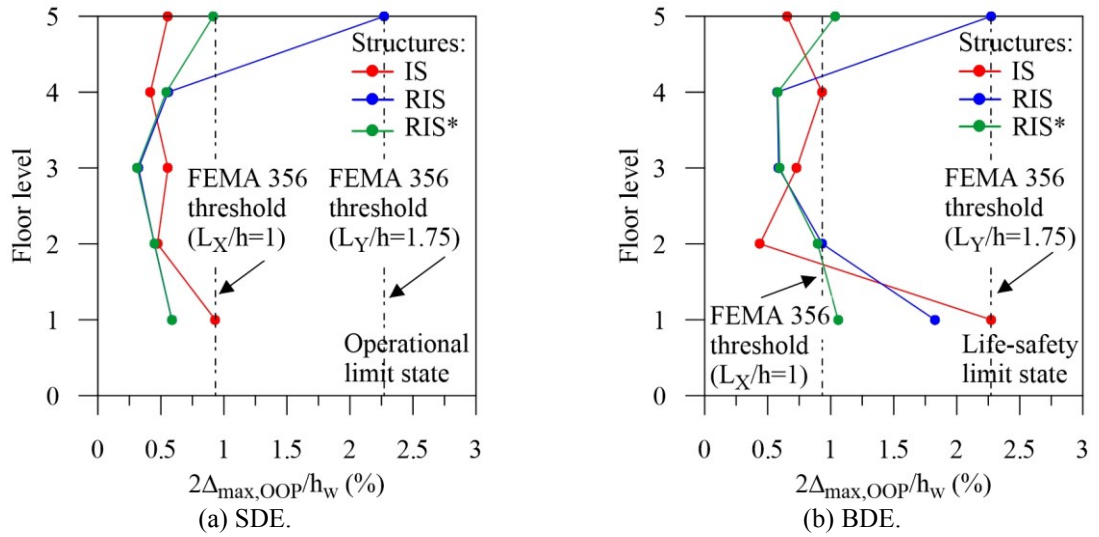

(a) SDE. (b) BDE.

Figure 6: Maximum OOP drift ratio of MIs for the original (IS) and retrofitted (RIS and RIS*) hospitals at serviceability and ultimate limit states.

Afterwards, IP and OOP collapse of MIs is analysed at the SDE and BDE for the original IS (Figure 7) and retrofitted RIS (Figure 8) and RIS* (Figure 9) hospitals. This corresponds to the attainment of residual strength in the IP and OOP force-displacement laws of MIs, without considering IP↔OOP mutual interaction. Results at the SDE highlight almost completely in-plane undamaged MIs (see grey box) in both principal directions (Figures 7a,b), while exten-

sive IP collapse (see blue boxes from the second to the fourth floor) are observed at the BDE (Figures 7c,d). Moreover, limited OOP collapses (see red box) are observed at the first floor considering the X (SDE, Figure 7a) and Y (BDE, Figure 7d) directions. It is worth noting that a different type and distribution of damage is obtained for the retrofitted IS. Specifically, only OOP collapse of MIs are resulted at the top floor considering SDE (Figure 8b) and BDE (Figures 8c,d). This kind of behaviour can be interpreted observing that the overall increase of lateral stiffness resulting from the insertion of the HYDBs produces an increase of the OOP acceleration of MIs at the top floor although there is a supplementary energy dissipation source. However, it should be noted that a high level of uncertainty about the geometrical and mechanical properties of MIs needs also to be accounted. In order to avoid too conservative results in terms of damage to façades, in Figure 9 reference is made to upper bound OOP force-displacement laws of MIs (RIS*), highlighting that undamaged OOP behaviour can be obtained at all levels when HYDBs are added.

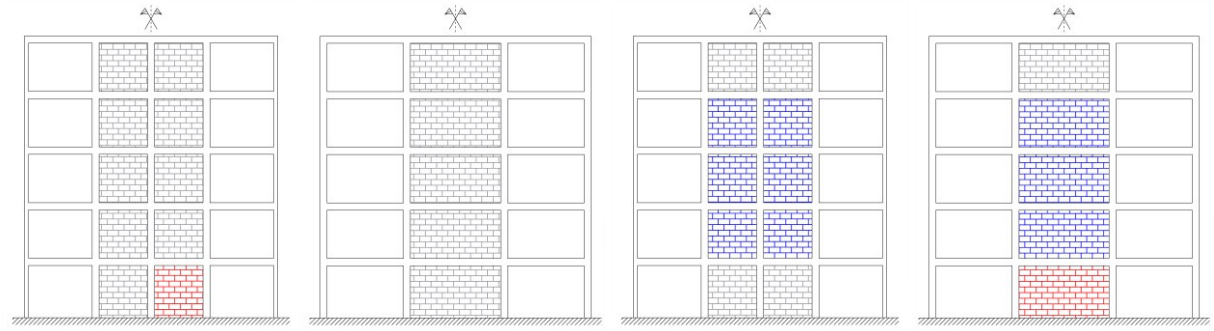

(a) SDE: X direction. (b) SDE: Y direction. (c) BDE: X direction. (d) BDE: Y direction.

Figure 7: In-plane (blue) and out-of-plane (red) collapse mechanisms of MIs for the original (BS) hospital.

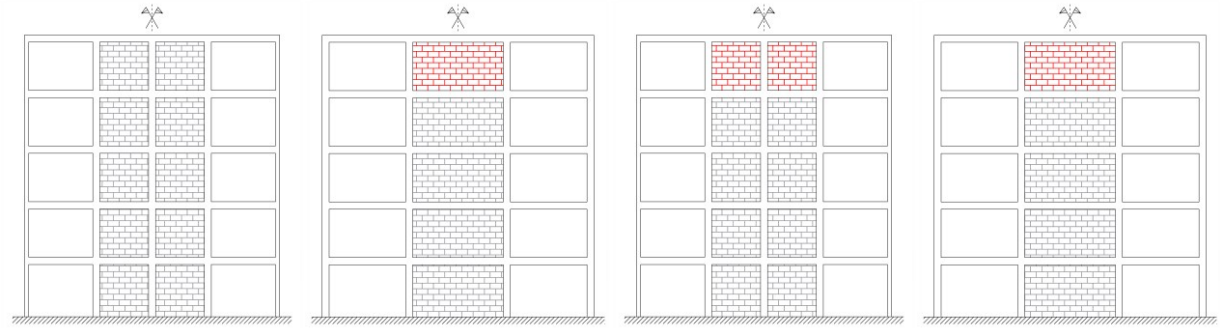

(a) SDE: X direction. (b) SDE: Y direction. (c) BDE: X direction. (d) BDE: Y direction.

Figure 8: In-plane (blue) and out-of-plane (red) collapse mechanisms of MIs for the retrofitted (RIS) hospital.

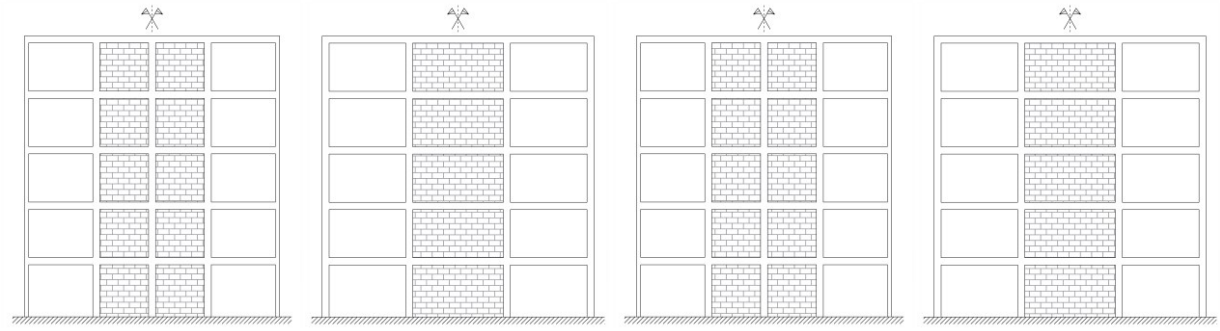

(a) SDE: X direction. (b) SDE: Y direction. (c) BDE: X direction. (d) BDE: Y direction.

Figure 9: In-plane (blue) and out-of-plane (red) collapse mechanisms of MIs for the retrofitted (RIS*) hospital.

Finally, with a view to analysing structural damage of the original and retrofitted structures, maximum values of the radial drift ratio, defined as radial drift of columns resulting from bi-axial seismic loads ($\Delta_{r,max}$) normalized by the storey height (h), and ductility demand of HYDBs ($\mu_{DB,max}$), placed along the perimeter, are plotted in Figures 10 and 11, respectively. The original BS and IS structures exhibit an irregular distribution law of the radial drift ratio with higher deformability at the intermediate levels where NTC18 threshold is not satisfied for SDE (Figure 10a) and BDE (Figure 10b). The insertion of the HYDBs generally ensures a significant reduction of the radial drift demand, with an almost constant distribution along the building height, the values being far below the NTC18 threshold. Ductility demand of the HYDBs confirms that their activation happens at the SDE (Figure 11a), so preventing non-structural IP and OOP collapse of MIs, while the ultimate value ($\mu_{DB,u}$=25) is never reached at BDE (Figure 11b), so resulting able to control the structural drift and effective in reducing the IP drift and OOP acceleration of MIs. Significant differences of $\mu_{DB,max}$ are observed at the top floor between RIS-Y and RIS*-Y, depending on OOP collapse of MIs (Figure 11b).

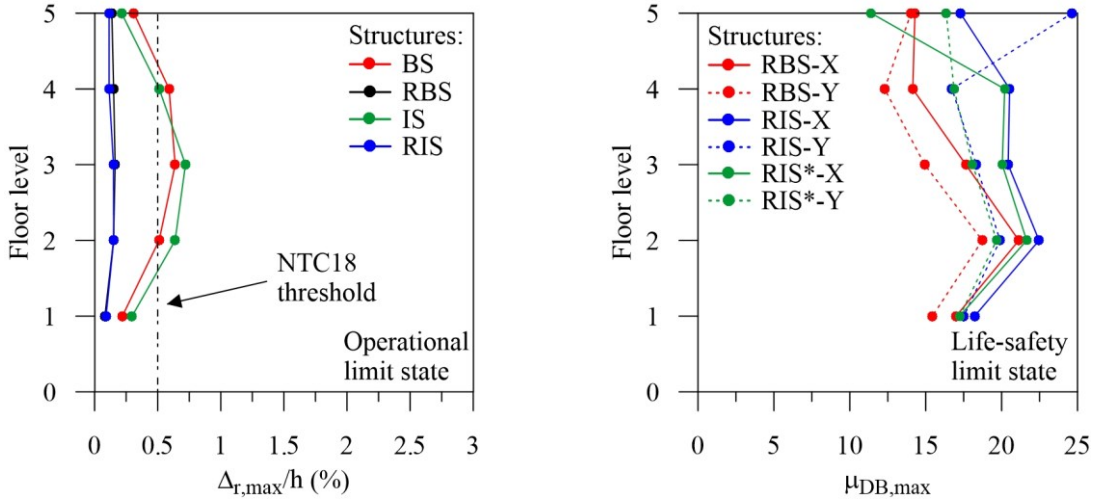

(a) SDE. (b) BDE.

Figure 10: Maximum radial drift ratio of the original (BS and IS) and retrofitted (RBS and RIS) hospitals at serviceability and ultimate limit states.

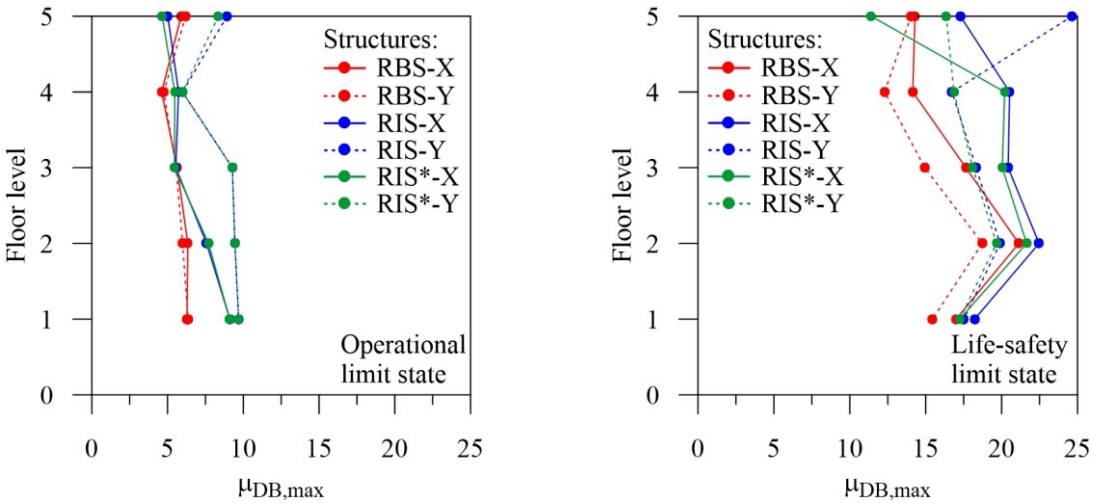

(a) SDE. (b) BDE.

Figure 11: Maximum ductility demand of HYDBs of the bare (RBS) and retrofitted (RIS and RIS*) hospitals at serviceability and ultimate limit states.

5 CONCLUSIONS

A Displacement-Based Design (DBD) procedure of hysteretic damped braces is updated in order to take into account the IP and OOP nonlinear response of masonry infills. To this end, a C++ computer code for the nonlinear static analysis of RC three-dimensional infilled framed structures is implemented, considering a five-element macro-model of MIs comprising four diagonal OOP nonlinear beams and one central IP nonlinear truss. The DBD procedure is applied for the seismic retrofitting of an RC framed structure located in Avellino (Italy), representing a pavilion of a hospital building originally designed for a medium-risk seismic zone. The variability of the OOP mechanical properties and aspect ratios of MIs is also investigated. Finally, nonlinear dynamic analyses are carried out for the serviceability (SDE) and Basic (BDE) Design Earthquakes in order to assess the reliability of the proposed methodology.

ACKNOWLEDGEMENTS

The present work is financed by Re.L.U.I.S. (Italian network of university laboratories of earthquake engineering), in line to the Convenzione D.P.C.-Re.L.U.I.S. 2022-2024, WP15, Code Contributions for Isolation and Dissipation.

REFERENCES

[1] F. Braga, V. Manfredi, A. Masi, A. Salvatori, Performance of non-structural elements in RC buildings during the L'Aquila 2009 earthquake. *Comput. Methods in Appl. Mech. Eng.*, **9**, 307-324, 2011.

[2] F. Mazza, In-plane-out-of-plane non-linear model of masonry infills in the seismic analysis of r.c.-framed buildings. *Earthq. Eng. Struct. Dyn.*, **48**(4), 432-453, 2019.

[3] F. Mazza, Modelling and nonlinear static analysis of reinforced concrete framed buildings irregular in plan. *Eng. Struct.*, **80**, 98-108, 2014.

[4] F. Mazza, A. Donnici, In-plane-out-of-plane single and mutual interaction of masonry infills in the nonlinear seismic analysis of RC framed structures. *Eng. Struct.*, **257**(5), 114076, 2022

[5] FEMA 356, Prestandard and Commentary for the Seismic Rehabilitation of Buildings. Washington, DC: Federal Emergency Management Agency, 2000.

[6] J.L. Dawe, C.K. Seah, Out-of-plane resistance of concrete masonry infilled panels. *Can. J. Civ. Eng.*, **16**(6), 854-864, 1989.

[7] F. Mazza, In-plane and out-of-plane nonlinear seismic response of masonry infills for hospitals retrofitted with hysteretic damped braces. *Soil Dyn. Earthq. Eng.*, **148**, 106803, 2021.

[8] F. Mazza, Displacement-based seismic design of hysteretic damped braces for retrofitting in-plan irregular r.c. framed structures. *Soil Dyn. Earthq. Eng.*, **66**, 231-240, 2014.

[9] DM96, Norme tecniche per le costruzioni in zone sismiche e relative istruzioni. D. M. 16-01-1996 and C.M. 10-04-1997, Italian Ministry of Public Works, Rome, Italy.

[10] Seismoartif Seismosoft, A computer program for generation of artificial accelerograms. Available from url www.seismosoft.com; 2019.

[11] NTC18, Norme tecniche per le costruzioni e relative istruzioni. D.M. 17-01-2018 and C.M. 11-02-2019, Italian Ministry of the Infrastructures and Transports, Rome, Italy.

[12] R.J. Mainstone, Supplementary note on the stiffness and strength of infilled frames. Current Paper CP 13/74, Building Research Station, U.K. 1974.

[13] S.H. Bertoldi, L.D. Decanini, C. Gavarini. Telai tamponati soggetti ad azioni sismiche, un modello semplificato: confronto sperimentale e numerico. *Atti del sesto Convegno Nazionale "L'Ingegneria Sismica in Italia"*, **2**, 815-824, 1993.

[14] G. Mucedero, D. Perrone, R. Monteiro, Nonlinear static characterisation of masonry-infilled RC building portfolios accounting for variability of infill properties. *Bull. Earthq. Eng.*, **19**, 2597-2641, 2021.

[15] Eurocode 8, Design of structures for earthquake resistance, Part 1: General rules, seismic actions and rules for buildings, EN 1998-1, European Committee for Standardisation, Brussels, Belgium.